

# Novel Effects of *Rosa damascena* Extract on Memory and Neurogenesis in a Rat Model of Alzheimer's Disease

Ebrahim Esfandiary,<sup>1</sup>\* Mohammad Karimipour,<sup>1</sup> Mohammad Mardani,<sup>1</sup>  
Hojjatallah Alaei,<sup>2</sup> Mustafa Ghannadian,<sup>3</sup> Mohammad Kazemi,<sup>4</sup>  
Daryoush Mohammadnejad,<sup>5</sup> Nasrin Hosseini,<sup>2</sup> and Abolghasem Esmaeili<sup>6</sup>\*

<sup>1</sup>Department of Anatomical Sciences and Molecular Biology, Isfahan University of Medical Sciences, Isfahan, Iran

<sup>2</sup>Department of Physiology, Isfahan University of Medical Sciences, Isfahan, Iran

<sup>3</sup>Pharmaceutical Sciences Research Center, Faculty of Pharmacy, Isfahan University of Medical Sciences, Isfahan, Iran

<sup>4</sup>Department of Genetic, Isfahan University of Medical Sciences, Isfahan, Iran

<sup>5</sup>Electron Microscopy Research center, Drug Applied Research Center, Tabriz University of Medical Sciences, Tabriz, Iran

<sup>6</sup>Cells, Molecular Biology and Biochemistry Division, Department of Biology, Faculty of Sciences, University of Isfahan, Isfahan, Iran

The number of older people who are suffering from memory impairment is increasing among populations throughout the world. Alzheimer's disease (AD) affects about 5% of people over 65 years old. The hippocampus, a brain area critical for learning and memory, is especially vulnerable to damage in the early stages of AD. Emerging evidence suggests that loss of neurons and synapses are correlated with dementia in this devastating disease. Therefore, neurogenesis and synaptogenesis in adulthood could serve as a preventive as well as a therapeutic target for AD. This study investigated the effect of *Rosa damascena* extract on neurogenesis and synaptogenesis in an animal model of AD. Molecular, cellular, and behavioral experiments revealed that this treatment could induce neurogenesis and synaptic plasticity and improve memory in AD. Our study suggests that *R. damascena* is a promising treatment for mild memory impairments and AD. © 2014 Wiley Periodicals, Inc.

**Key words:** neurogenesis; synaptogenesis; *Rosa damascena*; Alzheimer's disease

Alzheimer's disease (AD) is a progressive neurodegenerative disorder among the elderly, which is clinically manifested by cognitive and memory impairment, progressive decline of daily activities, and a variety of neuropsychiatric symptoms and behavioral disturbances. It has been estimated that 5% of the population older than 65 years is affected by AD (Cummings, 2004; Mattson, 2004). This devastating disorder is believed to start with synaptic dysfunction and subsequent loss of neuronal cells in the hippocampus and entorhinal cortex (Lacor et al., 2004). With respect to adult neurogenesis and synaptogenesis in rodent and human brains (Gould et al., 1999; Gage, 2000; Gross, 2000), it appears that the replacement

of lost neurons could represent a therapeutic approach for management of AD (Brinton and Wang, 2006). It is well accepted that neurogenesis constitutively occurs throughout adulthood within the two different neurogenic areas of the brain, the subventricular zone (SVZ) and the dentate gyrus (DG) of the hippocampus (Ming and Song, 2005; Lledo et al., 2006). Newly formed neurons integrating in the granule layer of the DG are thought to play a role in hippocampus-dependent forms of learning and memory. In addition, neurogenesis is thought to modulate brain plasticity and repair, by providing neurotrophic support for neurons and a pool of neural progenitor cells (NPC) with the capacity to differentiate into neurons, astrocytes, and oligodendrocytes (Jagasia et al., 2006; Zhao et al., 2008). Previous studies have demonstrated that behavioral and physiological stimuli such as learning (Gould et al., 1999), physical activity and voluntary wheel running exercise (van Praag et al., 1999; Brown et al., 2003), and environmental enrichment (Kempermann et al., 1997b; van Praag et al., 2000; Gage, 2002) as well as pharmacological agents such as antidepressants and antioxidants enhance hippocampal neurogenesis (Malberg

Contract grant sponsor: Isfahan University of Medical Sciences

\*Correspondence to: Ebrahim Esfandiary, Department of Anatomical Sciences and Molecular Biology, Isfahan University of Medical Sciences, Isfahan, Iran, Email: esfandiari@med.mui.ac.ir, or Abolghasem Esmaeili, Cell, Molecular Biology and Biochemistry Division, Department of Biology, Faculty of Sciences, University of Isfahan, Isfahan, Iran. E-mail: aesmaeili@sci.ui.ac.ir

Received 1 August 2013; Revised 18 September 2013; Accepted 26 September 2013

Published online 2 January 2014 in Wiley Online Library (wileyonlinelibrary.com). DOI: 10.1002/jnr.23319

et al., 2000) and synaptogenesis (Geinisman et al., 2001; Hajszan et al., 2005). Synapses are sites of cell–cell contacts that transmit electrical or chemical signals in the brain. Dendritic spines are protrusions on dendritic shaft where excitatory synapses are located. Synapses and dendritic spines are dynamic structures whose plasticity is thought to underlie learning and memory. Information can be stored in the brain by multiple synaptic mechanisms, including altered structure and chemistry of existing synapses, formation of new synapses, or elimination of old ones. Such synaptic plasticity is thought to be fundamental to learning and memory in the brain (Yu and Lu, 2012). Structural reorganization or remodeling (synaptic plasticity) is essential for maintenance of adequate brain function (Van Reempts et al., 1992). The important contribution of structural plasticity to various behavioral learning situations highlights the importance of connectivity remodeling and synapse stabilization as substrates for learning processes and memory retention (Caroni et al., 2012). Also structural plasticity is important to restore brain function following lesions (Caroni et al., 2012).

There have been promising developments in the area of herbal medicines as sources for new therapies for dementia. Experimental reports suggest that some herbs may have neuroprotective effects against amyloid- $\beta$  (Park and Kim, 2002; Kim et al., 2007). *Rosa damascena* (*R. damascena*) is a plant that belongs to genus *Rosa* and the family Rosaceae. Rosaceae are well known as ornamental plants and have been referred to as the king of flowers. Some of members of the Rosaceae family have long been used for food and medical purposes. Most studies have shown that *R. damascena* is a natural plant with a high level of flavonoids, including quercetin, myricetin, gallic acid, rutin, and kaemferol, and secondary active metabolites may have a curative effect as treatment for AD. Moreover, it is demonstrated that physiological functions of the *R. damascena* may be partially attributed to the abundance of flavonoids (Schiber et al., 2005; Kumar et al., 2008, 2010). Flavonoids comprise the most common group of polyphenolic compounds in the human diet and are found ubiquitously in plants (Manach et al., 2004). Several studies have indicated the consumption of flavonoid-rich plant foods and extracts may also be capable of inducing improvements in cognitive performance (Commenges et al., 2000; Spencer, 2008). The potential of flavonoids to improve neurological health seems to be related to their ability to interact with intracellular neuronal and glial signaling pathways, to influence the peripheral and cerebral vascular system, and to reduce neuronal damage and neuroinflammation process. It has been revealed that flavonoids upregulate antioxidant enzymes, the expression of proteins including brain-derived neurotrophic factor (BDNF), nerve growth factor (NGF), transcription factor of cyclic AMP response element binding protein (CREB), and early growth response protein-1 (ERG-1, or Zif268) involved in synaptic plasticity and also through their potential to protect vulnerable neurons, enhance existing neuronal function, stimulate neuronal regeneration, and induce neurogenesis (Williams et al., 2004; Dinges, 2006; Mann et al., 2007;

Spencer, 2009, 2010). Therefore, with respect to beneficial effects of *R. damascena* on behavioral performance, the present study sought to investigate the potential therapeutic effect of the *R. damascena* extract on learning and memory impairment in a rat model of AD via stimulation of adult neurogenesis and synaptic plasticity mechanisms. Also, because atrophy of memory-related medial temporal structures, particularly the hippocampal formation, is one of the earliest macroscopic hallmarks of the AD based on autopsy and neuroimaging studies (Killiany et al., 2000; Hampel et al., 2010), we used unbiased stereological study to measure the total volume of the hippocampus and absolute volume of its subfields in all groups and possible reverse effect of the *R. damascena* extract on decline-associated volumes.

## MATERIALS AND METHODS

### Animals

Male Wistar rats (200–250 g) were housed four per cage and maintained on a 12-hr light–dark cycle in an air-conditioned constant-temperature ( $23^{\circ}\text{C} \pm 1^{\circ}\text{C}$ ) room, with food and water available ad libitum. The Ethics Committee for Animal Experiments at Isfahan University of Medical Sciences approved the study, and all experiments were conducted in accordance with the international guiding principles for biomedical research involving animals (revised 1985). Initially, all animals were randomly divided into six groups ( $n = 10$ ) for evaluation of baseline training performance in the Morris water maze test. After the spatial acquisition phase of Morris water maze test, animals were grouped as follows: 1) control, 2) sham, 3) AD + normal saline, 4) AD + 300 mg *R. damascena* extract, 5) AD + 600 mg *Rosa damascena* extract, and 6) AD + 1,200 mg *Rosa damascena* extract. The protocol for their experimental design is summarized in Figure 1.

### Morris Water Maze Test

Spatial learning and memory were assessed by using Morris water maze behavioral test according to method of Morris, with minor modifications. Spatial acquisition phase of the Morris water maze was performed before the initiation of experiments (Morris et al., 1982).

The water maze test apparatus (Fig. 1B) was a circular water tank (180 cm in diameter and 60 cm high) made of dark gray stainless steel that was partially filled with water ( $24^{\circ}\text{C} \pm 2^{\circ}\text{C}$ ) and was surrounded by a variety of extramaze cues. The tank was divided into four equally spaced quadrants (northeast, northwest, southwest, and southeast), and four start positions were located at the intersections of the quadrants. A platform (12.5 cm in diameter and 38 cm high) was submerged 2 cm below the water surface in the northeast quadrant (target quadrant). The platform remained in the same quadrant during the training period and was then removed at the time of the probes task. The rats were required to find the platform using only distal spatial extramaze cues such as racks, a window, a door, bookshelves, and pictures that were available in the testing room. Twenty-four hours prior to the start of training, rats were habituated to the pool by allowing them to perform a 60-sec swim without the platform. In the spatial acquisition phase

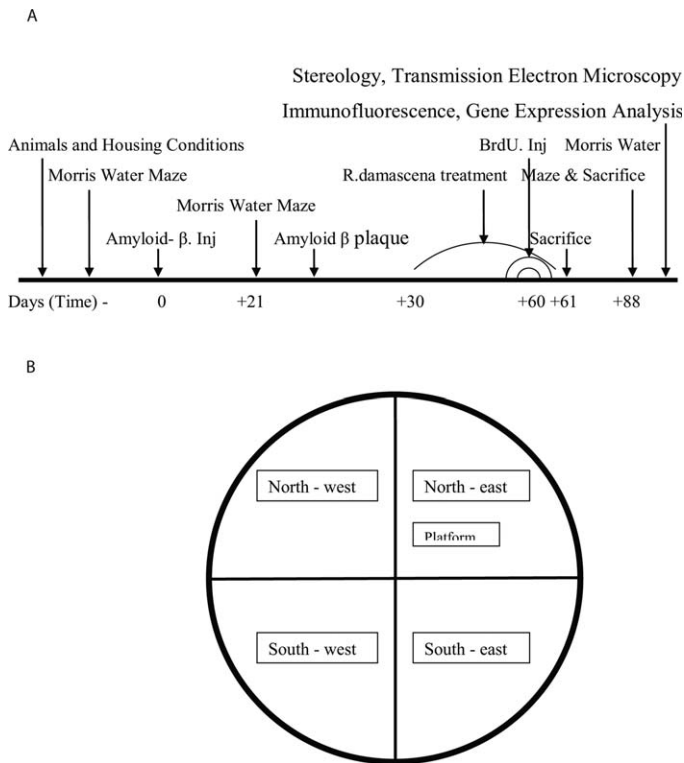


Fig. 1. **A:** Experimental schedule for the research design during the course of study. **B:** Schematic diagram of the tank and site of the platform.

(training phase), each rat participated in 20 trials, which were organized into five blocks of four trials (one trial/start position within a block). Each block was considered a separate test session, and trials were separated by 10 min. Animals had four trials per day for 5 successive days (acquisition trials), during which three parameters were evaluated, the time latency to reach the platform, the distance traveled, and the swimming speed. Rats were placed gently with their face to the wall in water. During each trial, the rat was given 60 sec to find the hidden platform. After mounting the platform, the animals were allowed to remain there for 30 sec and were then placed in a holding cage for 10 min until the start of next trial. If the rat failed to find the platform within 60 sec, it was gently guided to the platform and allowed to stay on it for 30 sec. After completion of training, to test possible deficits in sensorimotor processes, including swimming ability, motivation, and visual ability in the cued acquisition phase of the Morris water maze, rats were tested in the maze with a visible platform in a new location (southeast quadrant) on the final day of training. The test with the visual platform does not require special orientation and was used to show possible deficits in sensorimotor processes. For the test, the target platform was placed inside the pool 1 cm above the water line. Rats were allowed to swim for 60 sec. After completion of this phase, rats were gently dried with a towel, kept warm for 1 hr, and returned to their home cages until the initiation of the retention phase (probe trials) on the test days. In probe trials, the percentage time in the target quadrant was calculated. During the different versions of the maze, animals were monitored by a digital camera fixed 80 cm

above the maze, and different parameters were analyzed in software (Radiab1).

**Preparation of Amyloid-β<sub>1-42</sub> and Stereotaxic Surgery**

Amyloid-β<sub>1-42</sub> (Sigma, St. Louis, MO) was dissolved in phosphate-buffered saline (PBS; 0.1 M), and aliquots at a concentration of 1 μg/1 μl were stored at -20°C until use. For induction of aggregation, aliquots of amyloid-β<sub>1-42</sub> were incubated for 5 days at 37°C before administration.

Rats (third to sixth groups) were anesthetized intraperitoneally with chloral hydrate diluted in physiological saline (350 mg/kg). The animals subsequently were placed into a stereotaxic apparatus (Stoelting, Kiel, WI) with the head held horizontally. A heating pad was used to maintain body temperature at 36.5°C ± 0.5°C. A midline incision was made into the scalp, which was retracted, and the related area was cleaned and dried. In addition, lidocaine and epinephrine solution (0.4 ml) were injected in several locations surrounding the incision. Small holes were then drilled into the skull above the injection sites using a dental burr. The stereotaxic coordinates to conduct a bilateral microinjection in the CA1 region of the hippocampus (incisor bar -3.3 mm, anterior-posterior [AP] = -3.6 mm, medial-lateral [ML] = ±2.4 mm from the bregma and dorsal-ventral [DV] = 2.8 mm from top of the skull) were standardized from the stereotaxic atlas of Paxinos and Watson (2007). Microinjections were performed with a 30-gauge injector cannula. Polyethylene tubing (PE-10) was used to attach the injector cannula to a 5-μl Hamilton syringe. The flattened-tipped injector cannula was lowered into the bilateral hippocampus, and 3 μg/3 μl Aβ<sub>1-42</sub> was delivered slowly at a rate of 1 μl / min using a microinjection pump. The needle was kept in place for 5 min to allow the injected solutions and tissue to equilibrate and avoid possible reflux through the needle track. Incisions were ligated with silk thread. In the sham group, the same surgery was performed except that PBS was injected into CA1. No surgery was performed in control group. After surgery, animals were placed in heated chambers in a darkened room and allowed to recover with free access to food and water. Histological study was performed to confirm the correct injected area (data not shown).

Twenty-one days after operation, the first probe trial of the Morris water maze was performed, and memory impairment was confirmed in groups 3-6. For evaluation of amyloid-β plaques and deposits in the brain of rats, histological analysis was performed.

**Rat Brain Tissue for Histological and Amyloid β Plaque Analysis**

Immediately after the first probe trial of the Morris water maze test, one rat from each group was transcardially perfused (under deep anesthesia with chloral hydrate, 350 mg/kg/body weight, IP) with cold saline (~15 min until recovery of clear perfusion solution), followed by 4% paraformaldehyde (in 0.1 M phosphate buffer, pH 7.4). After complete perfusion, brain tissue including the hippocampus was immediately removed and postfixed overnight at 4°C with the same fixative solution. After histological processing, paraffin-embedded tissue sections were stained with Congo red.



Modified Highman's Congo red stain was used to identify amyloid deposits in the brain sections. Briefly, brain sections mounted on slides were subjected to the following staining steps: hydrated in water (5 min), stained in Congo red solution (0.5% in 50% ethanol) for 15–20 min, rinsed in distilled water, quickly differentiated (5–10 dips) in alkaline alcohol solution, rinsed in tap water (1 min), counterstained with Gill's hematoxylin (30 sec), rinsed in tap water (2 min), dehydrated with 95% and 100% ethanol, cleared in xylene, and finally coverslipped. With this protocol, amyloid deposits were stained red and the nuclei were blue (Fig. 2A,B).

### *R. damascena* Treatment

After the first probe trial of the Morris water maze, dried, standardized *R. damascena* extract (supplied by the Pharmaceutical Research Center, Isfahan University of Medical Sciences, Isfahan, Iran) was dissolved in normal saline 0.9% just before use and was administered orally at doses of 300, 600, and 1,200 mg/kg/day via a gastric tube in groups 4–6 for 1 month. Sham and third groups received only normal saline at the same time, but the control group did not receive anything. We considered that oral administration of *R. damascena* is crucial, because in traditional medicine *R. damascena* has always been taken orally. In addition, some herbs are known to be metabolized into active forms by intestinal absorption and then to exert pharmacological actions (Halliwell et al., 2000). Thus, nonoral administration of *R. damascena* may result in nonpharmacological artifacts.

### Bromodeoxyuridine Administration

The thymidine analog 5-bromo-2'-deoxyuridine (BrdU; Sigma) was dissolved at 10 mg/ml in 0.9% NaCl and sterile-filtered at 0.22  $\mu$ m. All animals received IP injections of 50 mg/kg body weight twice daily during the last 7 days of *R. damascena* treatment. One day after the last injection of BrdU, three animals from each group were perfused as described above to evaluate proliferation of the adult neural stem and progenitor cells (NPCs). To investigate adult neurogenesis, the remaining rats lived for an additional 4 weeks and were tested behaviorally. At the end of the 4 weeks, the rats were sacrificed as described above.

### Immunofluorescence Staining

After the second probe trial of the Morris water maze task, animals were anesthetized and transcardially perfused. Then, for paraffin embedding, tissues were first dehydrated in series of alcohols, cleared by incubations in xylene, and finally embedded in paraffin for 3–6 hr and then blocked. For histological studies, two series of coronal serial sections (5  $\mu$ m thickness) with 420- $\mu$ m intervals were obtained through the entire hippocampus by a rotary microtome (Leica, Vienna, Austria) resulting in two series of 12 coronal serial sections using systematic uniformly random sampling from each animal. The first series of sections was considered for stereological study and the second for immunofluorescence.

Twelve coronal serial sections from systematic uniformly random sampling through entire the length of the hippocampus were chosen for BrdU and BrdU-NeuN double labeling. The sections were mounted on poly-lysine-coated slides, dried overnight at 4°C temperature. In brief, the sections were first

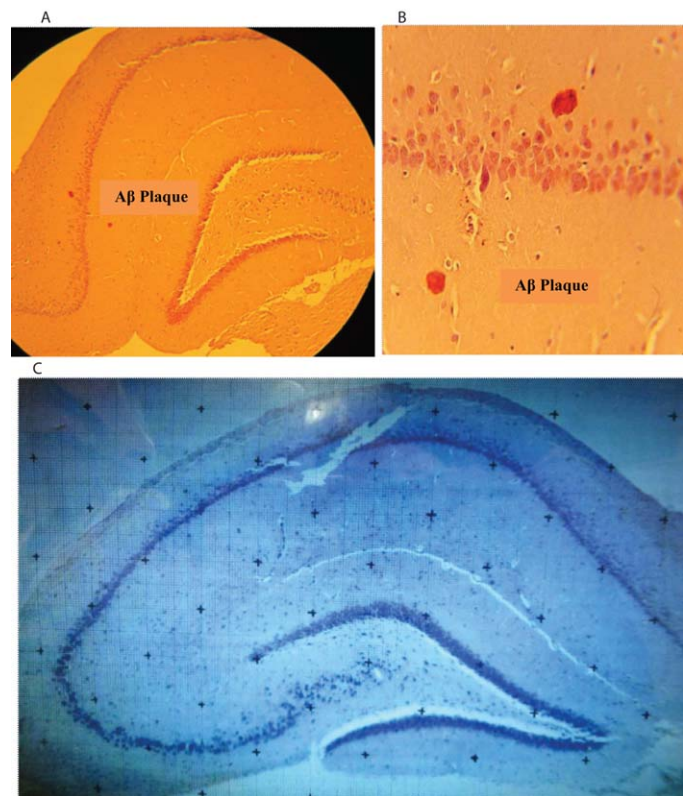


Fig. 2. **A,B:** Amyloid- $\beta_{1-42}$  deposits in rat hippocampus. **C:** Light micrograph of the rat hippocampus. Low-power photograph of a cresyl violet-stained horizontal section of the hippocampus with a lattice having a regular array of test points 40.2 mm apart. Ammon's horn consists of CA1, CA2, and CA3 pyramidal cell layer subdivisions, whereas the dentate gyrus consists of a molecular layer granule cell layer and the hilus. [Color figure can be viewed in the online issue, which is available at [wileyonlinelibrary.com](http://wileyonlinelibrary.com).]

deparaffinized and rehydrate in decreasing ethanol, then washed in Tris-buffered saline (TBS; 0.1 M Tris-HCl, pH 7.4, and 0.9% NaCl). For DNA denaturation, sections were incubated in a 2 N HCl bath for 60 min at 37°C, rinsed 10 min in 0.1 M boric acid, pH 8.5, and washed in TBS. Antigen retrieval was performed with incubation of sections in preheated 10 mM citrate buffer solution for 15 min at 100°C. For all experiments involving BrdU, DNA was denatured in 50% formamide and 50% 2 $\times$  standard saline citrate (2 $\times$  SSC is 0.3 M NaCl, 0.03 M sodium citrate, pH 7.0) at 65°C for 2 hr. Immunostaining for BrdU and NeuN was performed as described previously (Kempermann et al., 1997a). After several washes in TBS, sections were incubated in TBS 3% goat serum 0.3% Triton X (TBS++) for 30 min and then incubated for double labeling in a mixture of primary antibodies, including mouse anti-NeuN (Millipore, Chandlers Ford, Hants, United Kingdom; catalog No. MAB377; 1:100 in 0.3% Triton in TBS and 3% goat serum) and rat anti-BrdU (Accurate Chemical & Scientific, Westbury, NY; catalog No. OBT0030; 1:200 in 0.3% Triton with 3% goat serum) overnight at 4°C temperature. On the next day, after two washes with TBS, the sections were incubated in a mixture of secondary antibodies including Alexa

Fluor 568 goat anti-rat (catalog No. A-11077 [red; 1:200] and goat anti mouse Alexa Fluor 488 catalog No. A-11001 [green; 1:200] in 0.3% Triton in TBS with 3% goat serum) in a humid and dark chamber at room temperature for 1 hr and washed twice with TBS, and nuclear counterstaining was performed with 4',6'-diamidino-2-phenylindole dihydrochloride hydrate (DAPI; Sigma-Aldrich) for 3 min. After two washes with TBS, slides mounted with glycerol buffer, coverslipped, and then visualized with a fluorescence microscope and digitally photographed (Zeiss, AxioPhot, Germany). To investigate the proliferation of the neural stem cells and NPCs, the same protocol was used, but primary mouse anti-NeuN and secondary goat anti-mouse Alexa Fluor 488 were omitted.

### Gene Expression Analysis

The hippocampus was dissected from the brain immediately after decapitation and stored at  $-80^{\circ}\text{C}$  in RNAlater stabilization reagent until use. The frozen tissue was ground and used for the gene expression analysis. Total RNA was isolated by using the RNeasy Mini Kit with RNase-Free DNase Set (Qiagen, Valencia, CA) to ensure maximal removal of DNA during RNA purification. The RNA samples from three individual animals per group were used for synthesis of cDNA with a Revert AidTM First Strand cDNA Synthesis Kit (Fermentas; K1621, K1622) according to the manufacturer's recommendations. Relative gene expression analysis was performed with a Maxima SYBR Green/ROX qPCR Master Mix (2 $\times$ ) Kit (Fermentas; K0221) based on the manufacturer's recommendations. In each PCR, 10  $\mu\text{l}$  Power SYBR Green PCR Master Mix 2 $\times$  was mixed with 2  $\mu\text{l}$  cDNA and 10 pM/ $\mu\text{l}$  of each (forward and reverse) specific primer in a total volume of 20  $\mu\text{l}$ . Relative quantitative real-time PCR was performed using the Gene Amp 7500 Sequence Detection System (Applied Biosystems, Foster City, CA) with the following cycling parameters: 95 $^{\circ}\text{C}$  for 10 min, followed by 40 cycles of 95 $^{\circ}\text{C}$  for 15 sec, 60 $^{\circ}\text{C}$  for 1 min, followed by amplicon dissociation (95 $^{\circ}\text{C}$  for 15 sec, 60 $^{\circ}\text{C}$  for 1 min, increasing at 0.3 $^{\circ}\text{C}/\text{cycle}$  until 95 $^{\circ}\text{C}$  was reached). The endogenous control  $\beta$ -actin was used to normalize quantification of the mRNA target, and nonspecific amplifications were verified by a dissociation curve. All the reactions were performed in triplicate. Gene expression results were calculated using the delta delta cycle threshold ( $2^{-\Delta\Delta\text{Ct}}$ ) method. Primer sequences for BDNF, CREB, NGF, EGR-1, and  $\beta$ -actin were as follow. BDNF forward: 5'-GCCTCCTCTGCTCTTTCTG-3', BDNF reverse: 5'-TTATCTGCCGCTGTGACC-3'; NGF forward: 5'-TCCACCCACCCAGTCTTCCA-3', NGF reverse: 5'-TCACCTCCTTGCCCTTGATGTC-3'; CREB forward: 5'-AGTGACTGAGGAGCTTGTACCA-3', CREB reverse: 5'-TGTGGCTGGGCTTGAA C-3'; EGR-1 forward: 5'-GACCACCTTACCACCCACATCC-3', EGR-1 reverse: 5'-GCCTCTTGCGTTCATCACTCCT-3';  $\beta$ -actin forward: 5'-TGTCACCTTCCAGCAGATGT-3',  $\beta$ -actin reverse: 5'-GCTCAGTAACAGTCCGCC TAGA-3'.

### Unbiased Stereological Study

Sections were stained with the cresyle violet technique and used for stereological analysis. Anatomical boundaries of

the hippocampal formation and its subdivisions were distinguished under a light microscope according to the rat brain atlas and cell morphology (West et al., 1991; Paxinos and Watson, 2007). Because we worked with coronal brain sections, it was easier to distinguish the border between subfields. The hippocampus is composed of two regions, dentate gyrus (DG) and cornu ammonis (CA). The CA region is divided into subfields, CA1 contains small pyramidal cells. Field CA2 is characterized by a narrow, dense band of large pyramidal cells and field CA3 by a broad, loose band of large pyramidal neurons (Ragbetti et al., 2010; Zach et al., 2010). The Cavalieri principle was used as an estimator of volume. Thus, 12 sections were selected by using a systematic random sampling design and a random start for stereological estimations. By means of stereology software (Computer Assisted Stereological Toolbox [CAST] software) designed at our laboratory, the stereological probe (points) was superimposed on the images of the tissue sections viewed on the monitor. The volume was estimated using the following formula: Total volume (TV) =  $\Sigma P \cdot (a/p)d$ , where V (total) is the hippocampal volume,  $\Sigma P$  is the sum of the points falling on the section profile,  $a/p$  is the area associated with each point at the level of tissue section, and  $d$  is the distance between the sections sampled (see Fig. 5B–D). Volume density (Vv) of each subregion of the hippocampal formation was estimated by using point counting and the following formula:  $Vv = P(\text{layer})/P(\text{ref})$ , where  $P(\text{layer})$  and  $P(\text{ref})$  are the number of test points falling on the layer profile and on the reference space, respectively. The absolute volume (AV) of each subregion of hippocampus was estimated by multiplying the volume density (Vv) by the total volume (V) of the hippocampus to prevent the reference trap in according to following formula.  $AV = Vv(\text{layer}) \cdot V(\text{total})$  (Gundersen et al., 1988).

### Transmission Electron Microscopy

After the second probe trial of the Morris water maze, rats were deeply anesthetized and perfused as described above. The brain tissue including hippocampus was immediately removed and postfixed with 2% glutaraldehyde overnight at 4 $^{\circ}\text{C}$ , followed by 2% osmium peroxide, dehydration in an ascending series of ethanol concentrations, and finally impregnation in araldite resin and embedding. After orientation based on toluidine blue stain, blocks were trimmed to include the dentate gyrus. Semithin (450 nm thick) sections and ultrathin sections (60 nm silver-gold) were taken using a Leica Ultracut UCT ultramicrotome with a glass knife. Series of 12 ultrathin serial sections cut at a thickness of 60 nm per block were mounted with Formvar onto slotted copper grids, counterstained with uranyl acetate and lead citrate solutions, and observed in an electron microscope. Synapses in the dentate gyrus were imaged in the outer one-third of the stratum molecular. Stereology was performed as previously described (Sterio, 1984). Synapse density was determined by systematic random sampling on 50 disector pairs in each area, using the postsynaptic density as a counting unit. To analyze the proportion of multiple synapse boutons (MSBs), 100 synapses per area were fully reconstructed in three-dimensional space, and the proportion of MSBs synapses was calculated. MSBs were defined as

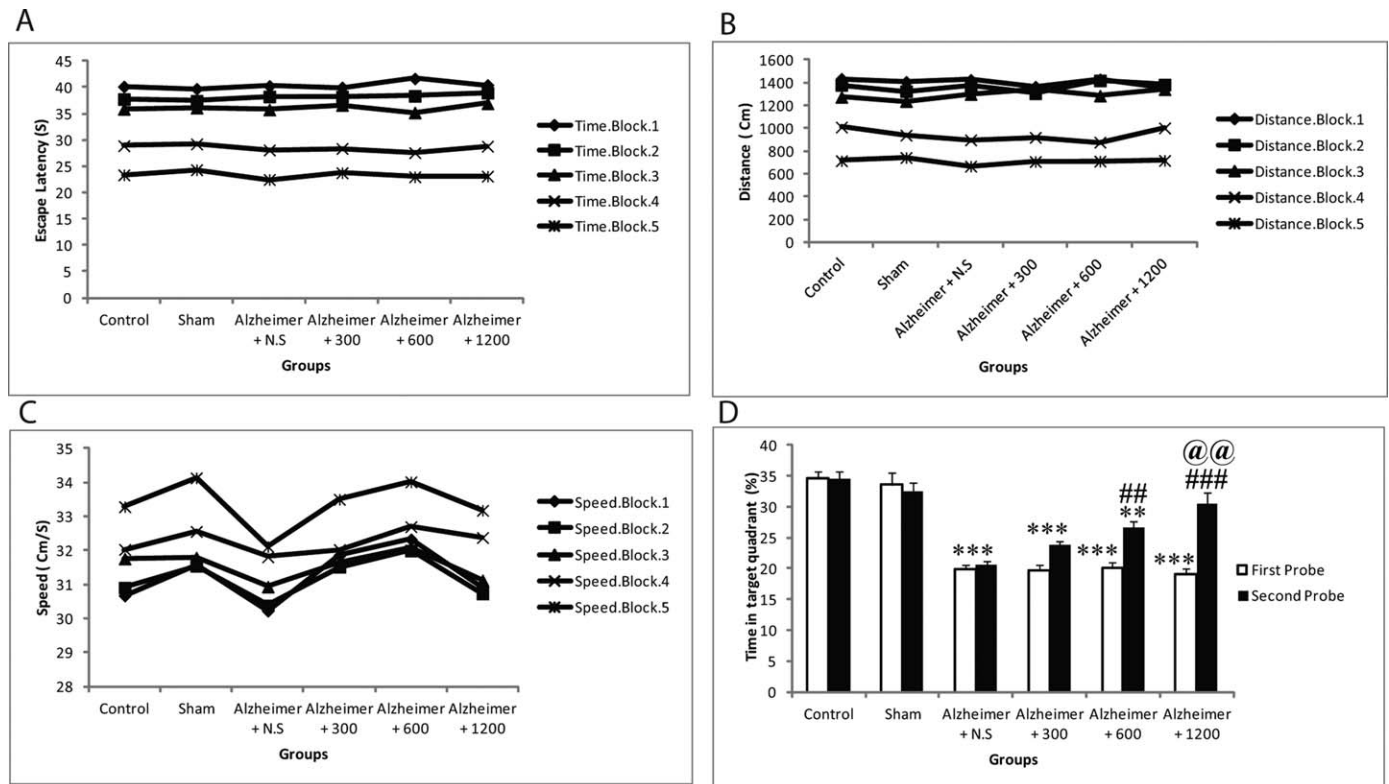


Fig. 3. A–D: Behavioral assessment of Morris water maze performance during the course of study. Spatial acquisition phase. **A:** In the spatial acquisition phase, there were no significant differences in blocks 1–5 among the six groups, but all rats showed a significant reduction in escape latency ( $P < 0.001$ ). **B:** Swimming distance ( $P < 0.001$ ) and increasing swimming speed ( $P < 0.001$ ); **C:** spatial retention phase (**D**). Data show that amyloid- $\beta$  injection had effects on spatial mem-

ory during the first probe trial as measured by mean percentage time in the target quadrant (D; white). *R. damascena* extract had significant effects on spatial memory during the second probe trial (percentage time in the target quadrant; D, black).  $**P < 0.01$ ,  $***P < 0.001$  different from the control and sham groups.  $##P < 0.01$ ,  $###P < 0.001$  different from the  $A\beta$ -injected group (Alz + NS).  $@@P < 0.01$  different from the  $A\beta$ -injected group (Alz + 300).

the synaptic contact between an axon terminal and more than one dendritic spine.

### Statistical Analysis

Data were expressed as mean  $\pm$  SEM and were analyzed in SPSS 19 software. Statistical analysis was performed by using the following tests. The escape latency, swim distance, and swim speed in the water maze were analyzed by two-way ANOVA. The probe trials data for percentage of time spent in the target quadrant were analyzed by multivariate ANOVA followed by Tukey's HSD test as a post hoc analysis. Results from the number of synapses were analyzed by Kruskal-Wallis/Mann-Whitney U-test. One-way ANOVA followed by Tukey's HSD multiple-comparisons tests as a post hoc analysis was performed for all other data.  $P < 0.05$  was considered statistically significant.

## RESULTS

### Learning Tests Before Administration of *R. damascena*

We tested learning performance in rats using spatial memory. To test spatial learning, we used the Morris

water maze task. The statistical analysis showed that there was no significant differences in mean time latency to find the hidden platform ( $F_{5,54} = 0.03$ ,  $P = 1 > 0.05$ ), mean swimming distance ( $F_{5,54} = 0.12$ ,  $P = 0.9 > 0.05$ ), or mean swimming speed ( $F_{5,54} = 0.53$ ,  $P = 0.7 > 0.05$ ) in blocks 1–5 of the spatial acquisition among all groups before application of amyloid- $\beta$ . However, significant differences in escape latency, swimming distance, and swimming speed among blocks in all groups (BLOCK effect  $F_{4,54} = 629.26$ ,  $P < 0.001$ ;  $F_{4,54} = 718.47$ ,  $P < 0.001$ ;  $F_{4,54} = 54.55$ ,  $P < 0.001$ ; respectively) were observed, indicating that spatial acquisition performance in all groups improved significantly during the training days (Fig. 3A–C).

### *R. damascena* Extracts Improved Spatial Learning and Memory Parameters

Multivariate ANOVA showed significant differences in the first probe trial among groups ( $P < 0.001$ ; Fig. 3D). Post hoc Tukey's HSD analysis showed that the mean percentage of time spent in the target quadrant in  $A\beta_{1-42}$ -injected groups (third to sixth groups) 21 days



after surgery was significantly decreased in comparison with control and sham groups ( $P < 0.001$ ), but no significant differences were demonstrated in mean percentage of time spent in the target quadrant between control and sham groups ( $P = 0.9$ ). These results showed that  $A\beta_{1-42}$  induced learning and memory impairment in the rats. Multivariate ANOVA showed that mean percentage of time spent in the target quadrant in the second probe trial after a 1-month administration of *R. damascena* extract was significantly increased among groups ( $P < 0.001$ ; Fig. 3D). Post hoc Tukey's HSD analysis showed that mean percentage of time spent in the target quadrant was significantly increased in extract-treated groups (fifth and sixth groups) relative to the third group, which received normal saline ( $P = 0.006$ ,  $P < 0.001$ , respectively), but mean percentage of time in the target quadrant in the fourth group did not significantly increase in comparison with the third group ( $P = 0.3$ ). Mean percentage of time in the target quadrant in the sixth group was significantly increased in comparison with group 4 ( $P = 0.002$ ). Taken together, these results show that *R. damascena* extract improved spatial learning and memory in a dose-dependent manner.

***R. damascena* Extract Stimulates Adult Neurogenesis in Hippocampus**

Neurogenesis is defined as the birth of new nerve cells and consists of a series of distinct steps, three of which can be examined separately: proliferation, survival, and differentiation. To compare the proliferation of adult neural stem cells and NPCs among all groups, we injected BrdU (50 mg/kg body weight), the proliferation marker, twice daily for 7 days, and analyzed BrdU incorporation 24 hr after the last injection. Post hoc Tukey's HSD analysis showed that the number of BrdU-positive cells was significantly increased in extract-treated groups (groups 4–6;  $2,107 \pm 19.68$ ,  $2,432 \pm 27.92$ ,  $2,703 \pm 10.41$ , respectively) relative to group 3 ( $1,987 \pm 21.46$ ,  $P < 0.001$ ; Fig. 4A–T). Thus the *R. damascena* extract increased the proliferation of the neural stem cells and NPCs in the hippocampus in all extract-treated groups. We next assessed the survival of BrdU-positive cells by comparing the number of BrdU-positive cells 4 weeks after the last injection with the number of labeled cells 24 hr after the last injection. The number of BrdU-positive cells after 4 weeks in all groups had significantly decreased relative to the number of labeled cells 24 hr after the last

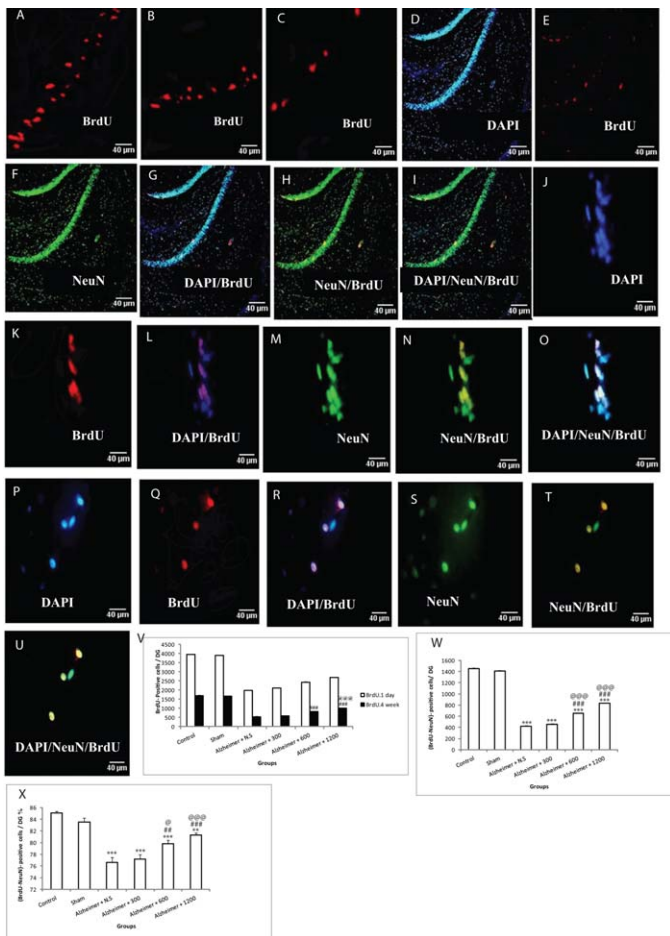


Fig. 4. A–R: Adult neurogenesis. Immunostaining of BrdU-positive cells in the dentate gyrus 1 day after the last BrdU injection (A–C). A: Control group. B: *Rosa damascena* extract. C: Alzheimer + NS. Sections were double labeled for BrdU (red), NeuN (green), and DAPI (blue). Colocalization was identified via immunofluorescence microscopy. D–O: Double immunostaining of BrdU- and NeuN-positive cells in the dentate gyrus 4 weeks after the last injection in an extract-treated group (Alz + 1,200). D: DAPI. E: BrdU. F: NeuN. G: DAPI/BrdU. H: NeuN/BrdU. I: DAPI/NeuN/BrdU. J: DAPI. K: BrdU. L: DAPI/BrdU. M: NeuN. N: NeuN/BrdU. O: DAPI/NeuN/BrdU. P–U: Double immunostaining of BrdU- and NeuN-positive cells in the dentate gyrus 4 weeks after the last injection in the control group. P: DAPI. Q: BrdU. R: DAPI/BrdU. S: NeuN. T: NeuN/BrdU. U: DAPI/NeuN/BrdU. V: Quantification of BrdU-positive cells in the DG 1 day and 4 weeks after the last BrdU injection. Data showed significant differences in the number of BrdU-positive cells at 1 day after the last BrdU injection among groups (P; white). Significant alterations after 4 weeks were also observed, but the number of BrdU-positive cells after 4 weeks was dose dependent (P; black).  $***P < 0.001$  different from the control and sham groups.  $###P < 0.001$  different from an  $A\beta$ -injected group (Alz + NS).  $@@@P < 0.001$  different from an  $A\beta$ -injected group (Alz + 300). W: Quantification of cells expressing NeuN relative to the total number of BrdU-positive cells per DG, 4 weeks after the last BrdU injection. Our results indicate that *Rosa damascena* extract significantly increased the number of NeuN-expressing cells relative to the total number of BrdU-positive cells in a dose-dependent manner.  $***P < 0.001$  different from the control and sham groups.  $####P < 0.001$  different from an  $A\beta$ -injected group (Alz + NS).  $@@@@P < 0.001$  different from an  $A\beta$ -injected group (Alz + 300). X: Quantification of BrdU-positive cells expressing NeuN in percentage of BrdU-positive cells per DG. The results showed that the number of BrdU- and NeuN-coexpressing cells in percentage of BrdU-positive cells was significantly increased in a dose-dependent manner.  $**P < 0.01$ ,  $***P < 0.001$  different from the control and sham groups.  $##P < 0.01$ ,  $###P < 0.001$  different from an  $A\beta$ -injected group (Alz + NS).  $@P < 0.05$ ,  $@@@P < 0.001$  different from an  $A\beta$ -injected group (Alz + 300). [Color figure can be viewed in the online issue, which is available at [wileyonlinelibrary.com](http://wileyonlinelibrary.com).]

injection, and post hoc Tukey's HSD analysis showed significant differences in number of BrdU-positive cells among all groups (Fig. 4). To assess the survival rate, we determined the ratio of labeled cells at 28 days with labeled cells at 24 hr after the last injection. We found that the survival rate of BrdU-positive cells in groups 3–6 was as 43.28%, 42.75%, 27.69%, 28.18%, 33.54%, 34.84%, respectively. Therefore, *Rosa damascena* could improve the survival rate of the newly generated neuronal cells in a dose-dependent manner, particularly at the middle and high doses. Finally, we examined the differentiation of BrdU-positive cells into neurons 4 weeks after the last injection by colabeling for BrdU and the neuron-specific marker NeuN (Fig. 4D–O). It was found that  $79.8\% \pm 0.62\%$  (group 5) and  $81.30\% \pm 0.39\%$  (group 6) of the surviving BrdU-positive cells expressed NeuN. Next, these results were compared with group 3 results ( $76.60\% \pm 0.84\%$ ), and a significant difference was observed in percentage NeuN-positive cells in groups 5 and 6 in comparison with group 3 but did not show any significant difference in percentage NeuN-positive cells between groups 3 and 4, indicating that differentiation was dose dependent. Surprisingly, although the low dose of *R. damascena* extract significantly increased BrdU-labeled cells 24 hr after the last injection ( $P < 0.05$ ), it did not have any effect on cell survival rate or differentiation of the adult neural stem cells and NPCs to mature neurons 4 weeks after the last injection ( $P > 0.05$ ). Altogether, these data indicate that adult rats in extract-treated groups 5 and 6 generate 67% and 77% more neurons per dentate gyrus than rats in group 3 (650, 831, and 421 cells, respectively;  $P < 0.001$ ; Fig. 4W,X). Thus, the *R. damascena* significantly increased adult neurogenesis in a dose-dependent manner.

### ***R. damascena* Extract Upregulates the Expression of BDNF, NGF, CREB, and EGR-1 (Zif268) Genes**

Neurotrophic factors including BDNF, NGF, and the transcription factor (CREB) are known to be involved in adult neurogenesis, neuroplasticity, synaptic plasticity, learning, and memory. EGR-1, or Zif268, has also been shown to be necessary for formation of different forms of long-term memory and to be expressed after synaptic activation, and it serves as a marker of synaptic functionality. For this reason, we decided to investigate whether *R. damascena* extract could modulate the expression of BDNF, NGF, CREB, and EGR-1. To test this, we measured expression of these genes by quantitative real-time RT PCR analysis. mRNA expression levels of BDNF, NGF, CREB, and EGR-1 were increased in extract-treated groups 5 and 6 in comparison with group 3 (Fig. 5A; BDNF 1.35- and 1.65-fold, 0.75,  $P < 0.001$ , NGF 1.25- and 1.56-fold, 0.84,  $P < 0.001$ , CREB 1.35- and 1.50-fold, 0.86,  $P < 0.001$ , and EGR-1 1.25- and 1.60-fold, 0.90,  $P < 0.001$ ). There were no significant differences in expression of genes between groups 3 and 4 ( $P > 0.05$ ) or between control and sham groups (Fig. 5A). Therefore, the expression of the mentioned genes

was dose dependent. These data indicate that *R. damascena* extract restores the reduced expression of BDNF, NGF, FRET, and EGR-1 genes in the rat model of AD.

### ***R. damascena* Extract Restored Decline-Associated Total Hippocampal Volume and Absolute Volumes of the DG and CA1**

Our results showed that TV.H was significantly increased in extract-treated groups (5 and 6) relative to group 3 ( $P = 0.003$ ,  $P < 0.001$ , respectively; Fig. 5) but TV.H in group 4, which received low-dose extract (300 mg/kg), was not significantly increased relative to group 3 ( $P = 0.5$ ). Also it was shown that AV (DG) and AV (CA1) in extract-treated groups (5 and 6) relative to group 3 were significantly increased ( $P = 0.01$ ,  $P < 0.001$ , and  $P = 0.001$ ,  $P < 0.001$ , respectively; Fig. 5C). However, group 4 did not show significant difference in AV (DG) and AV (CA1) relative to group 3 ( $P > 0.05$ ). Moreover, AV (CA2) and AV (CA3) in extract-treated groups were not significantly increased in comparison with group 3 ( $P > 0.05$ ; Fig. 5D). These results showed that *R. damascena* extract in a dose-dependent manner increased both total volume of hippocampus and absolute volume (DG, CA1), which were decreased under the influence of amyloid- $\beta$ .

### ***R. damascena* Extract Promotes Synaptic Plasticity and Remodeling**

To analyze extract-induced synaptic remodeling, we compared synapse ultrastructure among the all groups. Extract induced a significant increase in the proportion of MSB in the dentate gyrus in extract-treated groups (5 and 6) in comparison with group 3 ( $32.60\% \pm 0.40\%$ ,  $38.10\% \pm 0.43\%$ , and  $22.70\% \pm 1.10\%$ , respectively;  $P < 0.001$ ; Fig. 6A,B,D). Synapse density was also increased significantly in extract-treated groups in comparison with group 3 ( $2.20 \pm 0.20$ ,  $2.60 \pm 0.22$ , and  $1.40 \pm 0.16$ , respectively;  $P < 0.05$ ; Fig. 6C,E). In contrast, extract in low doses did not induce morphological modifications in the dentate gyrus from both aspects MSB and synapse density. Generally, these data showed that *R. damascena* enhances synaptic plasticity in a dose-dependent manner.

## **DISCUSSION**

Generation of new neurons is an important feature of the adult brain; in hippocampus, the newborn neuronal cells, governed by multiple factors, undergo complex stages of morphological and functional maturation and integrate into the existing neural circuitry (Ge et al., 2006). From a functional point of view, hippocampal neurogenesis plays an important role in memory processes. The use of endogenous neuronal precursors to replace lost and/or damaged cells has been proposed as a potential therapeutic approach for treatment of neurodegenerative disorders, including AD (Gage et al., 1998; Jin et al., 2004). In the present study, we investigated the hypothesis that the beneficial effect of *Rosa damascena* on dementia and



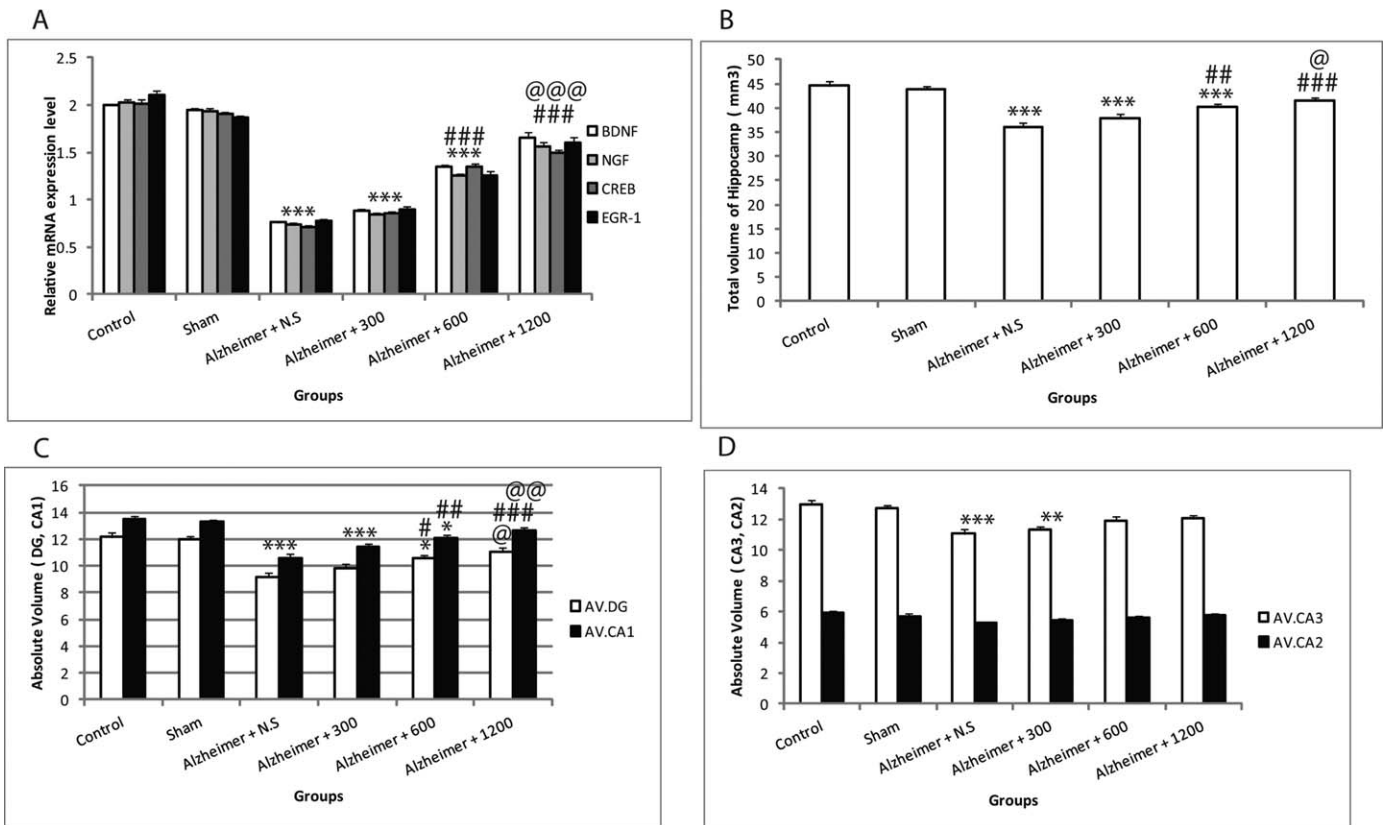


Fig. 5. **A:** Gene expression analysis. Data represent the average values obtained by quantitative real-time RT-PCR. Data showed significant differences in the expression of the BDNF, NGF, CREB, and Zif 268 (ERG-1) among groups. **\*\*\*** $P < 0.001$  different from the control and sham groups. **###** $P < 0.001$  different from an A $\beta$ -injected group (Alz + NS). **@@@** $P < 0.001$  different from an A $\beta$ -injected group (Alz + 300). **B–D:** Quantification of the total volume of the hippocampus and absolute volume of its subfields. **B:** Quantification of total

volume of the hippocampus. **C:** Absolute volume of the DG (white) and CA1 (black). **D:** Absolute volume of the CA3 (white) and CA2 (black). Our results indicate significant differences in TV (H) and AV (DG, CA1) among groups in a dose-dependent manner. **\*** $P < 0.05$ , **\*\*** $P < 0.01$ , **\*\*\*** $P < 0.001$  different from the control and sham groups. **#** $P < 0.05$ , **##** $P < 0.01$ , **###** $P < 0.001$  different from an A $\beta$ -injected group (Alz + NS). **@** $P < 0.05$ , **@@** $P < 0.01$ , different from an A $\beta$ -injected group (Alz + 300).

cognitive impairment of AD rats is mediated by enhanced adult neurogenesis and synaptic plasticity in the hippocampus. It has been reported that oral administration of *R. damascena* can relieve human stress and depression (Hongratanaworakit, 2009). It has also been shown that *R. damascena* extract causes outgrowth activity of neurite and suppresses A $\beta_{25-35}$ -induced atrophy and cell death.

Our results revealed that oral administration of *R. damascena* for 1 month rescues hippocampal-dependent learning and memory deficits in AD rats in a dose-dependent manner. *R. damascena* in its low dose (300 mg/kg) failed to produce any pronounced effect on the performance of rats in the tested task, whereas *R. damascena* in middle and high doses (600 and 1,200 mg/kg) produced significant effects. This dose-dependent effect may be explained by the difference in adult neurogenesis and synaptic plasticity mechanisms. Overall improvement of memory function was associated with increased proliferation of neural stem cells, adult neurogenesis, MSB, and synaptic density. Adult neurogenesis has been positively associated with spatial learning and memory performance

(Kee et al., 2007; Clelland et al., 2009; Garthe et al., 2009). The number and proliferation of neural stem cells at 24 hr after the last BrdU injection in all extract-treated groups were significantly increased in comparison with group 3, but the survival rate and differentiation of BrdU-positive cells into neurons in proliferating cells 4 weeks after the last BrdU injection in extract-treated groups were dose dependent. Therefore, a low dose of the *R. damascena* extract did not increase the survival rate and differentiation of newborn cells. Our results clearly show that the percentage of double-labeling cells (BrdU, NeuN) in extract-treated groups (5 and 6) was significantly more than in group 3. Double staining with BrdU and NeuN suggested that the increase in BrdU- and NeuN-coexpressing cells may be based mainly on an increase in neurogenesis and not on gliogenesis. Moreover, the spatial memory index correlated tightly with the number of BrdU/NeuN cells in extract-treated groups (5 and 6) and control and sham groups. This result is consistent with previous studies showing that spatial memory is associated with enhanced levels of hippocampal

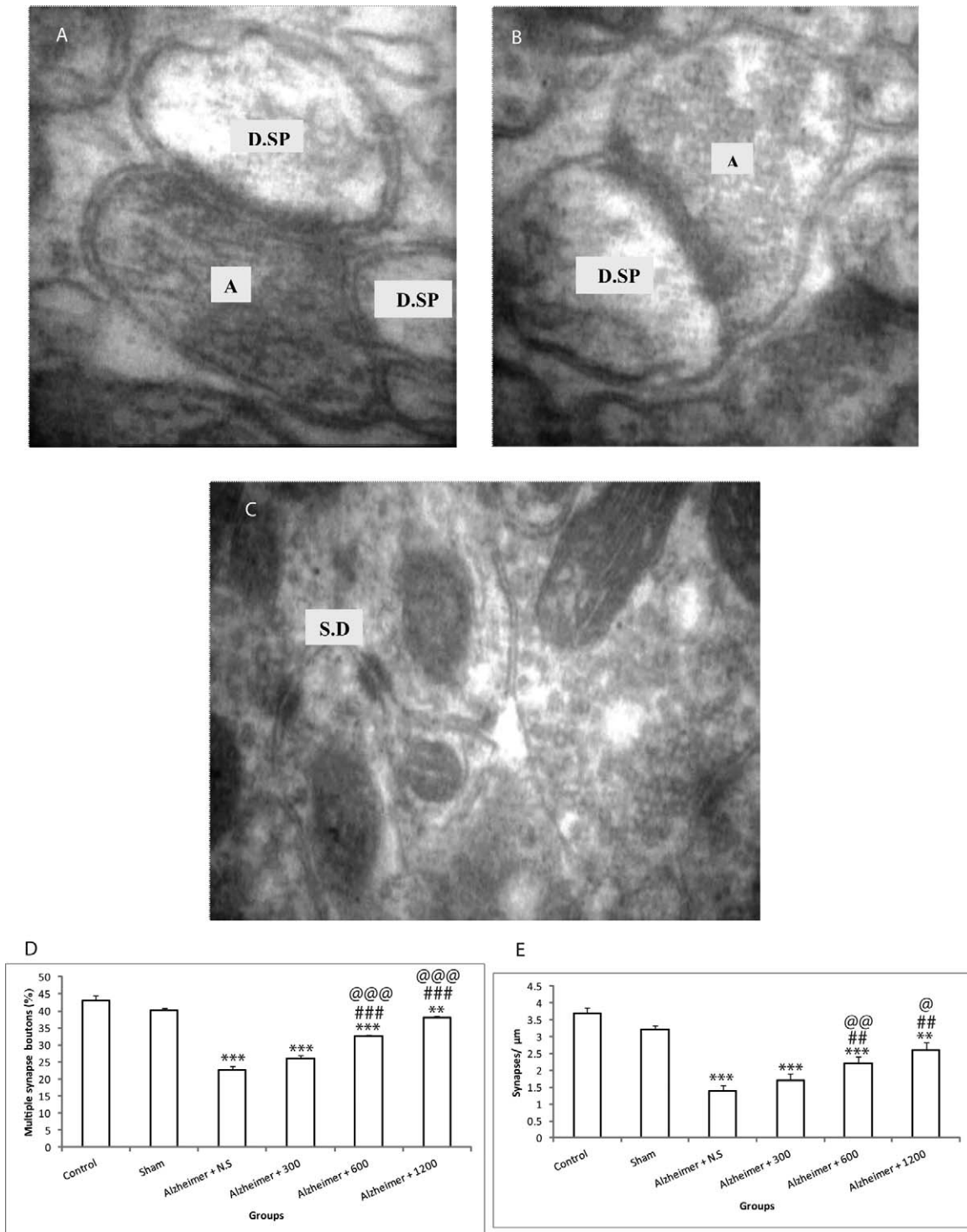


Fig. 6. A–E: Synapse ultrastructure and remodeling after treatment. **A:** Electron micrograph of a multiple-synapse bouton (MSB). **B:** Single-synapse bouton (SSB) showing axon terminals (A) making synaptic connections with dendritic spines (D.SP). **C:** Electron micrograph of a multiple-synaptic density. **D:** Proportion of dendritic spines contacting MSB in the dentate gyrus. **E:** Quantification of the synapse den-

sity in the dentate gyrus. Data show that the *Rosa damascena* extract significantly increased the proportion of MSB and synaptic density in a dose-dependent manner. **\*\*** $P < 0.01$ , **\*\*\*** $P < 0.001$  different from the control and sham groups. **#** $P < 0.05$ , **##** $P < 0.01$ , **###** $P < 0.001$  different from an A $\beta$ -injected group (Alz + NS). **@** $P < 0.05$ , **@@@** $P < 0.001$  different from an A $\beta$ -injected group (Alz + 300).

neurogenesis in rats (Drapeau et al., 2003). In our study, the most striking finding was that expression of BDNF, NGF, transcription factor CREB, and EGR-1 (Zif268) was significantly increased in extract-treated groups in comparison with group 3. Therefore, our results suggest that *R. damascena* extract enhances neurogenesis and synaptic plasticity by increasing the expression level of these genes. Neurotrophic factors such as BDNF and NGF are known to be implicated in adult neurogenesis, neuroplasticity, synaptic plasticity, and learning and memory (Poo, 2001; Lim et al., 2003). CREB is responsible for a variety of gene expressions essential for neuronal activities and synaptic functions related to learning and memory (Bonni et al., 1995; Lonze and Ginty, 2002). Quercetin as a flavonoid compound in *R. damascena* that stimulates dendrite formation and the expression of Zif268 in hippocampal neural cells. These processes could be mediated by phosphorylation of CREB (Miller and Kaplan, 2003). Although the mechanism of action of quercetin is unclear, the involvement of CREB in the regulation of neurogenesis, dendrite formation, Zif268 expression, and formation of dendritic spines underscores its importance in neuroplasticity and neuroprotective processes (Murphy and Segal, 1997; Bozon et al., 2002; Tully et al., 2003). Zif268 (EGR-1), may play a critical role in consolidation or stabilization of long-lasting memories, long-lasting synaptic plasticity, and spatial memory. This gene is expressed primarily after synaptic activation and therefore serves as a marker of synaptic functionality, and it has been shown to be necessary for the transition from short- to long-term synaptic plasticity and formation of different forms of long-term memory (Steiner and Kitai, 2000; Jones et al., 2001; Bozon et al., 2002; Guzowski, 2002; Jessberger and Kempermann, 2003).

Our study suggests that the increased neurogenesis induced by *R. damascena* is due to an increase in expression of neurotrophic factors and transcription factor CREB, cell proliferation, cell survival, and differentiation of neural stem cells to neurons. Therefore, *R. damascena*-induced neurogenesis may provide a mechanism through which *R. damascena* enhances cognitive performance in a dose-dependent manner. These findings underscore the ability of *R. damascena* to induce neurogenesis as compensation for the cell loss seen in AD. Pathologic and neuroimaging studies have shown that the memory-related medial temporal structures, especially the hippocampal formation, are particularly vulnerable to neuronal loss and atrophic changes during the course of AD (Bobinski et al., 1995, 1996; Convit et al., 1997; Killiany et al., 2000; Frisoni et al., 2010). We hypothesized that hippocampal volume and that of its subfields would be sensitive and specific indicators of AD neuropathology. There were two main findings in the stereological study. First, hippocampal volume loss in the AD disease process is regionally selective, so, in amyloid  $\beta$ -treated groups, the most prominent volume losses were found in dentate gyrus, CA3, and CA1, but absolute volume of the CA2 did not significantly decrease relative to control and sham groups. Overall, total volume of the hippocampus was significantly decreased in amyloid- $\beta$ -treated groups in

comparison with control and sham groups. Although there is general agreement that DG and CA1 are severely affected in AD, there is some controversy about the involvement of CA2 in AD (West et al., 1994; Bobinski et al., 1998; Fukutani et al., 2000; Redwine et al., 2003; Huang and Mucke, 2012). In the AD stage, the atrophic changes in CA1 become more pronounced, and the disease also spreads to the subiculum, resulting in a significant loss of total hippocampal volume. The pattern of hippocampal volume loss is also in agreement with findings of neuroimaging studies at 1.5 T, using surface mapping and shape analysis to make inferences about the pattern of hippocampal subfield volume loss in AD (Apostolova et al., 2006; Wang et al., 2006). Second, *R. damascena* reverses the decline in hippocampal volume and that of its subfields. Based on our results, *R. damascena* increased absolute volume of the DG and CA1 in a dose-dependent manner; however, the absolute volume of CA2 and CA3 were not significantly increased in extract-treated groups (5 and 6) in comparison with group 3. Overall, total volume of the hippocampus was significantly increased in extract-treated groups in a dose-dependent manner.

One of the mechanisms by which synaptic plasticity plays a role in the formation of new memories involves the learning-induced addition of new synapses on activated presynaptic terminals (Toni et al., 1999, 2001), resulting in the formation of MSB and the strengthening of activated synapses (Sorra and Harris, 1993; Shepherd and Harris, 1998). MSB result from the synaptogenesis induced by long-term potentiation (LTP; Toni et al., 1999) or associative learning (Geinisman et al., 2001). This form of synaptic plasticity is believed to play a role in the late phases of learning and to strengthen synaptic transmission between activated neurons (Lamprecht and LeDoux, 2004). *R. damascena* extract increased the proportion of MSB and synaptic density in the DG, suggesting that, under our experimental conditions, the DG was more involved in spatial learning. However, significant difference between groups 4 and 3 was not observed. This finding indicates that the effect of *R. damascena* on number of MSB and synaptic density was dose dependent. Structural plasticity is correlated with adult neurogenesis, suggesting that the function of new neurons may be mediated by an increase in synaptic remodeling. It has been shown that the flavonoids may act indirectly on the DG (Burke and Barnes, 2006). Also, it has been shown that these flavonoids significantly increased precursor cells proliferation in the DG in elderly rats (Casadesus et al., 2004). This correlation between DG neurogenesis, cognitive performance, and ageing is well documented (Kuhn et al., 1996; Kempermann et al., 1998; Drapeau et al., 2003). Flavonoids have a multiplicity of neuroprotective functions within the brain, including neural protection against neurotoxin injuries; neuroinflammatory suppression; and enhancement of memory, learning, and cognitive functions through the inhibition of apoptosis and promotion of neuronal survival, cerebrovascular blood flow, angiogenesis, neurogenesis, neuronal morphology, and synaptic plasticity. Furthermore, flavonoids prevent



neurodegeneration and brain aging via reduction of inducible nitric oxide synthase (iNOS), nitric oxide releasing, suppression of microglia and inflammatory cytokines such as tumor necrosis factor- $\alpha$  and interleukin-1 $\beta$ . Flavonoids activate the extracellular receptor kinase-cyclic AMP-response element-binding protein (ERK-CREB) pathway and the phosphatidylinositol-3 kinase-mammalian target of rapamycin (PI3-kinase-mTOR) or Akt/protein kinase B (PKB) cascade, leading to changes in synaptic plasticity and potentially angiogenesis/neurogenesis through the activation of endothelial nitric oxide synthase (eNOS) and the production neurotrophic factors, including BDNF, NGF, vascular endothelial growth factor (VEGF), and transforming growth factor- $\beta$ . On the other hand, flavonoids are known to inhibit proapoptotic signaling through inhibition of c-Jun N-terminal kinase (JNK) and apoptosis signal-regulating kinase 1 (ASK1). The inhibition of these kinases along with the activation of ERK1/2 leads to a suppression of apoptosis and neuroinflammation and thereby neuroprotection (Finkbeiner et al., 1997; Impey et al., 1998; Pham et al., 1999; Spencer, 2007, 2009). For example, quercetin is a flavonoid present in *R. damascena* that attenuates microglia- and/or astrocyte-mediated neuroinflammation (Chen et al., 2005). Also, through the activation CREB, quercetin regulates neuroplasticity and neuroprotective processes, including neurogenesis, synaptogenesis, synaptic remodeling, and formation of dendrites and dendritic spines (Murphy and Segal, 1997; Tully et al., 2003). For long-term clinical trials, it would be highly advantageous to investigate behavioral responses, under the influence of flavonoids, to changes in hippocampal volume and density, changes in neural stem cell and progenitor cell populations, molecular changes related to synaptic plasticity, and alterations in brain blood flow. Therefore, it appears that the consumption of flavonoid-rich foods and extracts throughout life might have the potential to limit or even reverse age-dependent deteriorations in memory and cognition and to delay the onset and progression of dementia.

### CONCLUSIONS

Our study shows that *R. damascena* enhances adult neurogenesis, hippocampal volume, and synaptic plasticity and finally reverses the A $\beta$ -associated memory abnormalities in a rat model of amyloid- $\beta$ -induced AD. Taken together, the diverse actions of individual natural components of *R. damascena* on adult neurogenesis and synaptic modification represent a new and promising method for generation of memory-enhancing drugs, although complementary experiments are still to be performed for better characterization of this valuable effect and its underlying mechanisms, in order to provide a basis for proper clinical trials.

### ACKNOWLEDGMENTS

The authors thank Azadeh Kabiri and Maryam Radahmadi, Department of Anatomical Sciences and Medical

Physiology, for their excellent technical assistance. None of the authors has a conflict of interest.

### REFERENCES

- Apostolova LG, Dinov ID, et al. 2006. 3D comparison of hippocampal atrophy in amnesic mild cognitive impairment and Alzheimer's disease. *Brain* 129:2867–2873.
- Bobinski M, Wegiel J, et al. 1995. Atrophy of hippocampal formation subdivisions correlates with stage and duration of Alzheimer disease. *Dementia* 6:205–210.
- Bobinski M, Wegiel J, et al. 1996. Neurofibrillary pathology—correlation with hippocampal formation atrophy in Alzheimer disease. *Neurobiol Aging* 17:909–919.
- Bobinski M, de Leon MJ, et al. 1998. Neuronal and volume loss in CA1 of the hippocampal formation uniquely predicts duration and severity of Alzheimer disease. *Brain Res* 805:267–269.
- Bonni A, Ginty DD, et al. 1995. Serine 133-phosphorylated CREB induces transcription via a cooperative mechanism that may confer specificity to neurotrophin signals. *Mol Cell Neurosci* 6:168–183.
- Bozon B, Davis S, et al. 2002. Regulated transcription of the immediate-early gene *Zif268*: mechanisms and gene dosage-dependent function in synaptic plasticity and memory formation. *Hippocampus* 12:570–577.
- Brinton RD, Wang JM. 2006. Therapeutic potential of neurogenesis for prevention and recovery from Alzheimer's disease: allopregnanolone as a proof of concept neurogenic agent. *Curr Alzheimer Res* 3:185–190.
- Brown J, Cooper-Kuhn CM, et al. 2003. Enriched environment and physical activity stimulate hippocampal but not olfactory bulb neurogenesis. *Eur J Neurosci* 17:2042–2046.
- Burke SN, Barnes CA. 2006. Neural plasticity in the ageing brain. *Nat Rev Neurosci* 7:30–40.
- Caroni P, Donato F, et al. 2012. Structural plasticity upon learning: regulation and functions. *Nat Rev Neurosci* 13:478–490.
- Casadesus G, Shukitt-Hale B, et al. 2004. Modulation of hippocampal plasticity and cognitive behavior by short-term blueberry supplementation in aged rats. *Nutr Neurosci* 7:309–316.
- Chen JC, Ho FM, et al. 2005. Inhibition of iNOS gene expression by quercetin is mediated by the inhibition of I $\kappa$ B kinase, nuclear factor-kappa B and STAT1, and depends on heme oxygenase-1 induction in mouse BV-2 microglia. *Eur J Pharmacol* 521:9–20.
- Clelland CD, Choi M, et al. 2009. A functional role for adult hippocampal neurogenesis in spatial pattern separation. *Science* 325:210–213.
- Commenges D, Scotet V, et al. 2000. Intake of flavonoids and risk of dementia. *Eur J Epidemiol* 16:357–363.
- Convit A, De Leon MJ, et al. 1997. Specific hippocampal volume reductions in individuals at risk for Alzheimer's disease. *Neurobiol Aging* 18:131–138.
- Cummings JL. 2004. Alzheimer's disease. *N Engl J Med* 351:56–67.
- Dinges DF. 2006. Cocoa flavanols, cerebral blood flow, cognition, and health: going forward. *J Cardiovasc Pharmacol* 47(Suppl 2):S221–S223.
- Drapeau E, Mayo W, et al. 2003. Spatial memory performances of aged rats in the water maze predict levels of hippocampal neurogenesis. *Proc Natl Acad Sci U S A* 100:14385–14390.
- Finkbeiner S, Tavazoie SF, et al. 1997. CREB: a major mediator of neuronal neurotrophin responses. *Neuron* 19:1031–1047.
- Frisoni GB, Fox NC, et al. 2010. The clinical use of structural MRI in Alzheimer disease. *Nat Rev Neurol* 6:67–77.
- Fukutani Y, Cairns NJ, et al. 2000. Neuronal loss and neurofibrillary degeneration in the hippocampal cortex in late-onset sporadic Alzheimer's disease. *Psychiatry Clin Neurosci* 54:523–529.
- Gage FH. 2000. Mammalian neural stem cells. *Science* 287:1433–1438.
- Gage FH. 2002. Neurogenesis in the adult brain. *J Neurosci* 22:612–613.
- Gage FH, Kempermann G, et al. 1998. Multipotent progenitor cells in the adult dentate gyrus. *J Neurobiol* 36:249–266.

- Garthe A, Behr J, et al. 2009. Adult-generated hippocampal neurons allow the flexible use of spatially precise learning strategies. *PLoS One* 4:e5464.
- Ge S, Goh EL, et al. 2006. GABA regulates synaptic integration of newly generated neurons in the adult brain. *Nature* 439:589–593.
- Geinisman Y, Berry RW, et al. 2001. Associative learning elicits the formation of multiple-synapse boutons. *J Neurosci* 21:5568–5573.
- Gould E, Beylin A, et al. 1999. Learning enhances adult neurogenesis in the hippocampal formation. *Nat Neurosci* 2:260–265.
- Gould E, Tanapat P, et al. 1999. Neurogenesis in adulthood: a possible role in learning. *Trends Cogn Sci* 3:186–192.
- Gross CG. 2000. Neurogenesis in the adult brain: death of a dogma. *Nat Rev Neurosci* 1:67–73.
- Gundersen HJ, Bendtsen TF, et al. 1988. Some new, simple and efficient stereological methods and their use in pathological research and diagnosis. *APMIS* 96:379–394.
- Guzowski JF. 2002. Insights into immediate-early gene function in hippocampal memory consolidation using antisense oligonucleotide and fluorescent imaging approaches. *Hippocampus* 12:86–104.
- Hajszan T, MacLusky NJ, et al. 2005. Short-term treatment with the antidepressant fluoxetine triggers pyramidal dendritic spine synapse formation in rat hippocampus. *Eur J Neurosci* 21:1299–1303.
- Halliwell B, Zhao K, et al. 2000. The gastrointestinal tract: a major site of antioxidant action? *Free Radic Res* 33:819–830.
- Hampel H, Frank R, et al. 2010. Biomarkers for Alzheimer's disease: academic, industry and regulatory perspectives. *Nat Rev Drug Discov* 9:560–574.
- Hongratanaworakit T. 2009. Relaxing effect of rose oil on humans. *Nat Prod Commun* 4:291–296.
- Huang Y, Mucke L. 2012. Alzheimer mechanisms and therapeutic strategies. *Cell* 148:1204–1222.
- Impey S, Smith DM, et al. 1998. Stimulation of cAMP response element (CRE)-mediated transcription during contextual learning. *Nat Neurosci* 1:595–601.
- Jagasia R, Song H, et al. 2006. New regulators in adult neurogenesis and their potential role for repair. *Trends Mol Med* 12:400–405.
- Jessberger S, Kempermann G. 2003. Adult-born hippocampal neurons mature into activity-dependent responsiveness. *Eur J Neurosci* 18:2707–2712.
- Jin K, Peel AL, et al. 2004. Increased hippocampal neurogenesis in Alzheimer's disease. *Proc Natl Acad Sci U S A* 101:343–347.
- Jones MW, Errington ML, et al. 2001. A requirement for the immediate early gene *Zif268* in the expression of late LTP and long-term memories. *Nat Neurosci* 4:289–296.
- Kalim MD, Bhattacharyya D, et al. 2010. Oxidative DNA damage preventive activity and antioxidant potential of plants used in Unani system of medicine. *BMC Complement Altern Med* 10:77.
- Kee N, Teixeira CM, et al. 2007. Preferential incorporation of adult-generated granule cells into spatial memory networks in the dentate gyrus. *Nat Neurosci* 10:355–362.
- Kempermann G, Kuhn HG, et al. 1997a. Genetic influence on neurogenesis in the dentate gyrus of adult mice. *Proc Natl Acad Sci U S A* 94:10409–10414.
- Kempermann G, Kuhn HG, et al. 1997b. More hippocampal neurons in adult mice living in an enriched environment. *Nature* 386:493–495.
- Kempermann G, Kuhn HG, et al. 1998. Experience-induced neurogenesis in the senescent dentate gyrus. *J Neurosci* 18:3206–3212.
- Killiany RJ, Gomez-Isla T, et al. 2000. Use of structural magnetic resonance imaging to predict who will get Alzheimer's disease. *Ann Neurol* 47:430–439.
- Kim DS, Kim JY, et al. 2007. Alzheimer's disease drug discovery from herbs: neuroprotectivity from beta-amyloid (1–42) insult. *J Altern Complement Med* 13:333–340.
- Kuhn HG, Dickinson-Anson H, et al. 1996. Neurogenesis in the dentate gyrus of the adult rat: age-related decrease of neuronal progenitor proliferation. *J Neurosci* 16:2027–2033.
- Kumar N, Bhandari P, et al. 2008. Reversed phase-HPLC for rapid determination of polyphenols in flowers of rose species. *J Separation Sci* 31:262–267.
- Lacor PN, Buniel MC, et al. 2004. Synaptic targeting by Alzheimer's-related amyloid  $\beta$  oligomers. *J Neurosci* 24:10191–10200.
- Lamprecht R, LeDoux J. 2004. Structural plasticity and memory. *Nat Rev Neurosci* 5:45–54.
- Lim KC, Lim ST, et al. 2003. Neurotrophin secretory pathways and synaptic plasticity. *Neurobiol Aging* 24:1135–1145.
- Lledo PM, Alonso M, et al. 2006. Adult neurogenesis and functional plasticity in neuronal circuits. *Nat Rev Neurosci* 7:179–193.
- Lonze BE, Ginty DD. 2002. Function and regulation of CREB family transcription factors in the nervous system. *Neuron* 35:605–623.
- Malberg JE, Eisch AJ, et al. 2000. Chronic antidepressant treatment increases neurogenesis in adult rat hippocampus. *J Neurosci* 20:9104–9110.
- Manach C, Scalbert A, et al. 2004. Polyphenols: food sources and bioavailability. *Am J Clin Nutr* 79:727–747.
- Mann GE, Rowlands DJ, et al. 2007. Activation of endothelial nitric oxide synthase by dietary isoflavones: role of NO in Nrf2-mediated antioxidant gene expression. *Cardiovasc Res* 75:261–274.
- Mattson MP. 2004. Pathways towards and away from Alzheimer's disease. *Nature* 430:631–639.
- Miller FD, Kaplan DR. 2003. Signaling mechanisms underlying dendrite formation. *Curr Opin Neurobiol* 13:391–398.
- Ming GL, Song H. 2005. Adult neurogenesis in the mammalian central nervous system. *Annu Rev Neurosci* 28:223–250.
- Morris RG, Garrud P, et al. 1982. Place navigation impaired in rats with hippocampal lesions. *Nature* 297:681–683.
- Murphy DD, Segal M. 1997. Morphological plasticity of dendritic spines in central neurons is mediated by activation of cAMP response element binding protein. *Proc Natl Acad Sci U S A* 94:1482–1487.
- Park SY, Kim DS. 2002. Discovery of natural products from *Curcuma longa* that protect cells from beta-amyloid insult: a drug discovery effort against Alzheimer's disease. *J Nat Prod* 65:1227–1231.
- Paxinos G, Watson C. 2007. The rat brain in stereotaxic coordinates: hard cover edition. San Diego: Academic Press.
- Pham TA, Impey S, et al. 1999. CRE-mediated gene transcription in neocortical neuronal plasticity during the developmental critical period. *Neuron* 22:63–72.
- Poo MM. 2001. Neurotrophins as synaptic modulators. *Nat Rev Neurosci* 2:24–32.
- Ragbetli MC, Aydinlioglu A, et al. 2010. Total neuron numbers in CA1–4 sectors of the dog hippocampus. *Indian J Med Res* 131:780–785.
- Redwine JM, Kosofsky B, et al. 2003. Dentate gyrus volume is reduced before onset of plaque formation in PDAPP mice: a magnetic resonance microscopy and stereologic analysis. *Proc Natl Acad Sci U S A* 100:1381–1386.
- Schiber A, Mihalev K, et al. 2005. Flavonol glycosides from distilled petals of *Rosa damascena* Mill. *Z Naturforsch C* 60:379–384.
- Shepherd GM, Harris KM. 1998. Three-dimensional structure and composition of CA3→CA1 axons in rat hippocampal slices: implications for presynaptic connectivity and compartmentalization. *J Neurosci* 18:8300–8310.
- Sorra KE, Harris KM. 1993. Occurrence and three-dimensional structure of multiple synapses between individual radiatum axons and their target pyramidal cells in hippocampal area CA1. *J Neurosci* 13:3736–3748.
- Spencer JP. 2007. The interactions of flavonoids within neuronal signaling pathways. *Genes Nutr* 2:257–273.
- Spencer JP. 2008. Flavonoids: modulators of brain function? *Br J Nutr* 99(E Suppl 1):ES60–ES77.
- Spencer JP. 2009. The impact of flavonoids on memory: physiological and molecular considerations. *Chem Soc Rev* 38:1152–1161.

- Spencer JP. 2010. The impact of fruit flavonoids on memory and cognition. *Br J Nutr* 104(Suppl 3):S40–S47.
- Steiner H, Kitai ST. 2000. Regulation of rat cortex function by D1 dopamine receptors in the striatum. *J Neurosci* 20:5449–5460.
- Sterio DC. 1984. The unbiased estimation of number and sizes of arbitrary particles using the disector. *J Microsc* 134:127–136.
- Toni N, Buchs PA, et al. 1999. LTP promotes formation of multiple spine synapses between a single axon terminal and a dendrite. *Nature* 402:421–425.
- Toni N, Buchs PA, et al. 2001. Remodeling of synaptic membranes after induction of long-term potentiation. *J Neurosci* 21:6245–6251.
- Tully T, Bourtchouladze R, et al. 2003. Targeting the CREB pathway for memory enhancers. *Nat Rev Drug Discov* 2:267–277.
- van Praag H, Kempermann G, et al. 1999. Running increases cell proliferation and neurogenesis in the adult mouse dentate gyrus. *Nat Neurosci* 2:266–270.
- van Praag H, Kempermann G, et al. 2000. Neural consequences of environmental enrichment. *Nat Rev Neurosci* 1:191–198.
- Van Reempts J, Dikova M, et al. 1992. Synaptic plasticity in rat hippocampus associated with learning. *Behav Brain Res* 51:179–183.
- Wang L, Miller JP, et al. 2006. Abnormalities of hippocampal surface structure in very mild dementia of the Alzheimer type. *Neuroimage* 30:52–60.
- West MJ, Slomianka L, et al. 1991. Unbiased stereological estimation of the total number of neurons in the subdivisions of the rat hippocampus using the optical fractionator. *Anat Rec* 231:482–497.
- West MJ, Coleman PD, et al. 1994. Differences in the pattern of hippocampal neuronal loss in normal ageing and Alzheimer's disease. *Lancet* 344:769–772.
- Williams RJ, Spencer JP, et al. 2004. Flavonoids: antioxidants or signaling molecules? *Free Radic Biol Med* 36:838–849.
- Yu W, Lu B. 2012. Synapses and dendritic spines as pathogenic targets in Alzheimer's disease. *Neural Plast* 2012:247150.
- Zach P, Mrzilkova J, et al. 2010. Delayed effects of elevated corticosterone level on volume of hippocampal formation in laboratory rat. *Physiol Res* 59:985–996.
- Zhao C, Deng W, et al. 2008. Mechanisms and functional implications of adult neurogenesis. *Cell* 132:645–660.